



Multi-objective Optimization of Shot-peening Parameters using Design of Experiments and Finite Element Simulation: A Statistical Model

Mahdi Hassanzadeh¹, Seyed Ebrahim Moussavi Torshizi²

¹ Faculty of Mechanical and Energy Engineering, Shahid Beheshti University, A.C., Tehran, Iran, Email: m_hassanzadeh@sbu.ac.ir

² Faculty of Mechanical and Energy Engineering, Shahid Beheshti University, A.C., Tehran, Iran, Email: e_moussavi@sbu.ac.ir

Received March 31 2020; Revised April 19 2020; Accepted for publication May 16 2020.

Corresponding author: S.E. Moussavi Torshizi, (e_moussavi@sbu.ac.ir)

© 2021 Published by Shahid Chamran University of Ahvaz

Abstract. Shot-peening is a mechanical surface treatment used extensively in the industry to enhance the performance of metal parts against fatigue. Thus, it is important to determine main parameters of shot-peening in order to obtain its optimal values. The purpose of this study is to achieve a statistical model to determine the important parameters of the shot-peening process by considering the effect of sample thickness on the responses and achieving the multi-objective optimal parameters. To do this, response surface methodology are used to determine the governing models between the response variable and the input parameters. Shot velocity, shot diameter, coverage percentage and sample thickness are selected as shot-peening parameters. Residual compressive stress, its depth and roughness are considered as the response variable. Using finite element analysis, shot-peening process are simulated. The desirability function approach is used for multi-objective optimization so that the optimal shot-peening parameters, which simultaneously provide two response variables in optimal mode, are obtained. The results show that surface stress and maximum residual stress are independent of shot velocity, whereas, the depth of the compressible stress and roughness are directly related to shot velocity. In addition, thickness modifies surface stress and the depth of the compressible stress. The optimal conditions for surface stress, maximum compressive stress, and roughness simultaneously with high-coverage and low-velocity can be achieved as well.

Keywords: Shot-peening, Finite element method, Design of experiments (DoE), Residual stresses, roughness.

1. Introduction

Shot-peening is frequently considered as an effective approach in enhancing the mechanical components behavior against fatigue [1-3]. The advantageous effects of the process to the surface hardening and the residual stresses field are stated in [2, 3]. The results of shot-peening are dependent on the mechanical features of the desired material and the circumstances of the process (shot type, shot velocity, coverage, impact angle, etc.). Sometimes, when the parameters of shot-peening are not chosen properly, one can see adverse effects on fatigue resistance [2, 3]. This issue demonstrates that the effect of shot-peening on the performance of fatigue is dependent on process parameters selection. Therefore, it is critical to estimate the shot-peening parameters impacts on the fatigue behavior of the metal pieces and to select it optimally and appropriately.

The shot-peening effects can be estimated using of numerical, analytical, and experimental approaches. Hills et al. [4], Al-Obaid [5], and Al-Hassani [6] presented analytical approaches to estimate the shot-peening residual stress. The use of analytic approaches is encountered with restrictions; therefore, numerous empirical researches have been carried out on the shot-peening field. Obata et al. [7] and Dorr et al. [8] have investigated the contribution of shot velocity and size to surface roughness and residual stress to the surface. Ahmed [9] has recently investigated the effect of different parameters of shot-peening on the micro-hardness, residual compressive stress, corrosion behavior, and wettability behavior of steel AISI 316L. Through a completely factorial design technique, Mahagaonkar et al. [10] also investigated the effects of the exposure time, shot type, air pressure and nozzle distance and their interference impacts on steel micro-hardness. Nam et al. [11] also examined the effects of pressure, nozzle distance, exposure time, and impact angle on micro-hardness and residual compressive stress of aluminum 2124-T851 using response surface methodology.

In comparison with the experimental test, numerical simulation can be used to reduce time and costs. A single-shot contact model was simulated by Hong et al. [12]. They investigated the contribution of the parameters including impact velocity, shot diameter, material properties and impact angle to the distribution of residual stresses at the desired surface. Meguid et al. [13] have presented a symmetry model for a quarter of the shot in which the effect of single shot and two shot on the target surface has been studied. In order to investigate the contribution of major parameters such as shot size and velocity on Almen intensity and residual



stress, Guagliano [14] presented a finite element model with five-shot contact. Numerous shots impacts have been lately utilized for the simulation of shot-peening process to get results that are more realistic. Kim et al. [15], Cheng et al. [16] and Meguid et al. [17] have developed some ideal models with regular distribution of the shots. However, for the completely randomized distribution of shots, closer to the real shot-peening model in comparison with uniformly distributed models of shots, a number of models are developed by Ghasemi et al. [18], Miao et al. [19], and Mahmoudi et al. [20].

The optimal parameters of shot peening have been studied by researchers. Nam et al. [21] and AlSumait [22] have determined the optimal coverage of the maximum fatigue life. Petit-Renaud et al. [23] and Romero et al. [24] optimized the maximum compressive stress in the form of an objective function. George et al. [25] optimized the shot-peening intensity by using the Taguchi's approach. Vielma et al. [26] and Unal [27] considered roughness as an objective function to be optimized. Bhuvanaraghan et al. [28] investigated multi-objective shot-peening by genetic algorithm approach and optimized the compressive residual stress considering work hardening and roughness under certain limits. Baragetti [29] optimized the maximum compressive stresses and the surface roughness, the compressive residual stress depth and the maximum compressive stress depth, simultaneously. Unal et al. [30] optimized surface hardness and roughness, simultaneously. Seddik et al. [31] have managed to optimize two objective functions of damage variable and compressive residual stress for the shot-peening process. In general, there are a few studies dealing with multi-objective optimizations, in which multiple objective functions were examined simultaneously. Assuming the adverse effect of surface roughness on fatigue life, considering alongside with the residual stress in the shot-peening process may be a significant matter.

It has been observed that many studies have been carried out on the simulation of the shot-peening process, but insufficient researches have been conducted on statistical models. In the literatures, the statistical model has not been used to interpret and understand the shot-peening process. In addition, the relationship between numerical solution and experimental work has not been investigated. Furthermore, the effect of the thickness of the shot-peened sample has not been investigated on the responses so far. Consequently, these questions arise: Can a statistical model be used to better understand the shot-peening process and to select the optimal parameters? What is the effect of thickness on stresses, depth of compressive stress and roughness? How can the numerical models with experimental results be compared to each other? It is believed that the present study responds these questions more attentively.

This paper is aimed to extract the statistical model to investigate the significance of the parameters of shot-peening and optimize it with regard to surface roughness and residual compressive stress. The design of experiments are developed with three levels to evaluate the effect and interaction between various parameters and its impact on the features of the shot-peening surface. Design engineers can apply this analysis as an advantageous tool for shot-peening parameters optimization. The most important phases of the presented approach can be summarized as follows:

- (i) Development and improvement of a finite element model through a randomized repeated procedure of the shot impact
- (ii) DoE approach and numerical simulations
- (iii) Extraction of the statistical model and their interpretation through statistical methods
- (iv) Optimization of shot-peening circumstances on the basis of the two functions of surface roughness and residual stress.

2. Finite Element Model

The finite element method was used to calculate the displacements, stresses and other quantities. The simulation of shot-peening was done using the commercial code ABAQUS 2017. The explicit solver (explicit) was used to consider the dynamic effects of shot-peening. In order to automatically generate a model with specific inputs (shot-peening conditions, target material, boundary conditions, type of the shots and so on), the code was written based on the Python script. FEM analysis was developed using a damping coefficient [32] to reduce stress oscillations and avoiding uncontrolled oscillations after impact in the FEM model. The material damping was presented following Eq. 1.

$$D = \alpha M + \beta K \quad (1)$$

where D , M and K are the damping, mass and stiffness matrices, respectively. As a result of a number of trial runs, it was determined that effective damping can be achieved using a stiffness proportional damping coefficient $\beta = 2 \times 10^{-9} \text{ s}$. To obtain reliable values of mass proportional damping α , the following approach was adopted. The minimal modal frequency ω_0 could be estimated as in Eq. (2).

$$\omega_0 = \frac{1}{H} \sqrt{\frac{2E}{\rho}} \quad (2)$$

where E is the target Young's modulus, ρ is its density and H is the thickness of the target. The mass proportional damping is then determined as in Eq. 3.

$$\alpha = 2\omega_0\xi \quad (3)$$

where ξ is the corresponding modal damping parameter. In this study, ξ was selected 0.5 to decay the unwanted low-frequency oscillations [33].

Thermal and spring-back effects are neglected because of the negligible impact on the results. The proposed 3D model predicts residual compressive stress, plastic deformation and surface integrity.

2.1 Boundary condition and geometry

In order to reduce the effect of the target edges, the target was modeled with dimensions of $6D \times 6D \times h$, where D is the diameter of the shot and h is the target thickness. The only central area with dimensions of $2D \times 2D$ in upper surface was encountered with multiple shots as is seen in Fig. 1. The target was meshed by eight-node linear brick solid elements with reduced integration C3D8R. To improve the accuracy and efficiency of the results, a fine-mesh grid arrangement $0.02\text{mm} \times 0.02\text{mm} \times 0.02\text{mm}$ for the shot peened area and a greater mesh size was considered for the rest of the body. All the target surfaces except the upper surface were fixed.



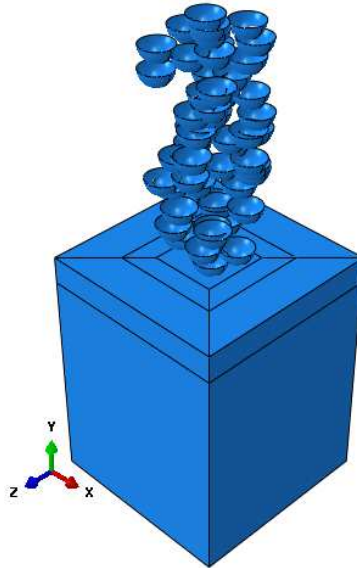


Fig. 1: A three-dimensional finite element model of shot-peening

2.2. Material model

The target material was AISI420 martensitic stainless steel and Johnson-Cook model was considered to simulate this material (Eq. 4).

$$\sigma = (A + B(\epsilon^p)^n) \left(1 + C \log \left(\frac{\dot{\epsilon}^p}{\dot{\epsilon}_0} \right) \right) \left(1 - \left(\frac{T - T_r}{T_m - T_r} \right)^m \right) \quad (4)$$

where A , B , C , n and m are the constants of the material obtained by mechanical tests. The parameters ϵ^p , $\dot{\epsilon}^p$, $\dot{\epsilon}_0$, T_r , T_m and T are the equivalent plastic strain, the plastic strain rate, the reference strain rate, the room temperature, the melting temperature and reference temperature, respectively. Johnson Cook's parameters and other material parameters for AISI420 are presented in Tables 1 and 2. The shots were considered rigid.

2.3. Shot stream simulation

Most of the mentioned shots are perpendicular to the surface. The following basic parameters were similarly assigned to the whole shots: velocity in V_y direction, diameter (D), the friction between the shots and the target surface by the Columbian friction model (Eq. 5):

$$F_f = \mu F_n \quad (5)$$

here, F_n is the normal force, F_f is the friction force, and μ is the friction coefficient. The friction coefficient for the contact between the shots and the target was chosen as 0.2, since the results of residual stress will not change much for a friction coefficient larger than 0.2 according to the literature [34,35]. The number of shots is associated with the shot size, the coverage percentage, and the level of impact.

In case the shots hit the target successively, the time required for simulation is $N\Delta t$, where N is the quantity of shots and Δt is the time interval between the impacts; however, in case a number of shots simultaneously hit the target surface, the whole simulation time is decreased. For this reason, several rows were assumed for the shots, each of which spaced from the surface proportional to the impact time. The origin of the coordinates was placed at the center of the target surface so that the y -axis was perpendicular to the surface. The shots position in $x-z$ plane varied randomly from one row to another to generate a random impact condition. Therefore, the total time needed for simulation is only $N_y \Delta t$, where N_y is the number of shots rows that is less than N in accordance with the number of shots per plane. The modeling phases were as following:

- (1) A local coordinate system is created at the center of the material surface, so that the y -axis remains perpendicular to the surface.
- (2) By using the random function, the center coordinates j -th shot ($j \geq 1$) is generated in k -th row:

Table 1: Johnson–Cook parameters for the AISI 420 steel material

A(MPa)	B(MPa)	C	n	m	$T_r(^{\circ}C)$	$T_m(^{\circ}C)$	$\dot{\epsilon}_0$
450	738	0.02	0.388	0.8	27	1454	1

Table 2: Physical and mechanical parameters for the AISI 420 steel material

Density(g/cm ³)	Poisson's ratio	Young's Modulus(GPa)	Thermal Conductivity(W/m K)	Specific heat (J/kg $^{\circ}C$)	Thermal expansion (10 ⁻⁶ $^{\circ}C$)
7.8	0.3	200	24.9	460	10.3



$$\begin{aligned}x_{kj} &= \text{random.uniform}(-d, d) \\z_{kj} &= \text{random.uniform}(-d, d), & j = 1, \dots, N_s, k = 1, \dots, N_y \\y_{kj} &= (k-1)V\Delta t + d/2\end{aligned}\quad (6)$$

where, N_s is the number of shots for each row, and N_y is the number of rows of shots ($N_y = N / N_s$) $\text{random.uniform}(-d, d)$ is a random number created in the range $(-d, d)$ uniformly, Δt is the time interval between the successive shot hits, which is 3.5×10^{-6} s for our model, and d is the shot diameter.

(3) The distance between the center of the i -th shot and the center of the j -th shot ($i = 1 \dots j - 1$) determined through Eq. 7.

$$d_{i,j} = \sqrt{(x_j - x_i)^2 + (z_j - z_i)^2} \quad (7)$$

In case $d_{i,j} < d$, the shot j overlaps with the previous shot i , which is not possible physically. The shot j ought to be removed and return to step 2.

(4) Go back to step (2) to generate the next shot center coordinates until the creation of the whole shots is finished.

2.4. Shot-peening coverage

The shot-peening coverage is described as the ratio of the shot area to the total surface area. In statistical sense, the coverage of 100% is obtained only when the target shot-peening is continued for an infinite time, whilst this overlap does not affect the coverage. Generally, coverage of 98% is roughly considered as 100%, and the coverage of 200% is described as twice as long as required to reach 100% [1]. Apparently, the shot-peening coverage has been generated on the basis of the dimple dimensions and the shot-peening time. One can use the Avrami equation to assess the coverage [36]:

$$C = 100\% \times (1 - e^{-nr^2Rt}) \quad (8)$$

where, C is the coverage, r indicates the mean dimple radius, and R is the number of shot hits in one second for the surface unit, t denotes the duration of shot-peening time. Obviously Rt indicates the whole number of shots.

3. Design of Experiments (DoE) and Response Surface Methodology (RSM)

3.1 Theory

The design of experiments includes a statistical approach for data gathering and prediction of the results on the basis of a limited number of inputs. This method is a systematic method for creating response surface as a function of input parameters. One can use RSM to analyze the experiment design results. When the whole independent variables are monitored and measurable during the test, the response process is presented in:

$$Y = f(x_1, x_2, \dots, x_k) \quad (9)$$

In Eq. 9, k shows the number of independent variables. It is essential to find a logical function for the association between the response and independent variables. Therefore, the second-order polynomial function shown in Eq. 10 is usually utilized in response surface methodology (RSM) [37]:

$$Y = \beta_0 + \sum_{i=1}^k \beta_i x_i + \sum_{i=1}^k \beta_{ii} x_i^2 + \sum_{i=1}^{k-1} \sum_{j=i+1}^k \beta_{ij} x_i x_j + \varepsilon \quad (10)$$

In Eq. 10, β_0 indicates the constant value, β_i shows the linear coefficients, β_{ii} denotes the second-order coefficients, β_{ij} indicates interaction coefficients, and ε is the model error. One can express Eq. 10 in the matrix form as Eq. 11:

$$Y = X \times B + \varepsilon \quad (11)$$

where ε is the vector of errors, Y represents the observation vector, B indicates the vector of the tuning parameters of the set, and X represents the matrix of the values of the design variables. Using the least squares regression, the regression coefficients are determined:

$$\hat{B} = (X^T X)^{-1} X^T Y \quad (12)$$

Thereafter, the fitted regression is determined by the following equation:

$$\hat{Y} = X \hat{B} \quad (13)$$

One can evaluate the goodness of fit using Eq. 14:

$$R^2 = 1 - \frac{\sum_i (Y_i - \hat{Y}_i)^2}{\sum_i (Y_i - \bar{Y}_i)^2} \quad (14)$$

where \hat{Y}_i , \bar{Y}_i , and Y_i are the approximate value, the mean, of the observed values, and the observed values, respectively.



Table 3: Input factors and their levels

Parameter	Notation	Level		
		-1	0	+1
Shot size (mm)	d	0.5842	0.7112	0.8382
Shot velocity (m/s)	V	70	90	110
Peening coverage (%)	C	100	150	200
Plate thickness (mm)	h	3	4.5	6

3.2 Shot-peening parameters and responses selection

In an experimental study commonly parameters such as pressure, Almen intensity, shot diameter and so on are selected. However, in the present study because of numerical simulation of shot peening process, the parameters such as shot size, shot velocity, coverage, and target thickness have been studied to link their effects on residual stress and roughness. Almen intensity is the criteria for measuring shot peening intensity. Almen intensity quantifies by a thin strip of SAE 1070 steel named Almen strip with dimensions of 76 mm×19 mm and three thicknesses. The thicknesses are 0.79 mm, 1.29 mm and 2.39 mm for type N, A and C respectively. Almen strips fixed by means of four bolts and shot-peening operation is performed with the same shot peening parameters and different exposure times. When the peened strip is released, it will curve. The arc heights of the curve are measured under different exposure times. The Almen intensity is defined as the arc height at saturation which is the point, on the curve of peening time versus arc height, beyond which the arc height increases by less than 10% when the exposure time doubles. According to the Fig. 2 [38] we can proposed that Almen intensity in the finite intervals is linear in relation to velocity. The residual stresses included the residual stresses of the target surface ($\sigma_{\text{surf}}^{\text{RS}}$) and the maximum induced residual stresses ($\sigma_{\text{max}}^{\text{RS}}$). In addition, the depths of the maximum residual stress ($\delta_{\text{max}}^{\text{RS}}$) and the compressive stress depth (δ_c^{RS}) are also considered in this study. For estimating the residual stress distribution, the average residual stress is calculated at each depth [39]:

$$\bar{\sigma}_{xx} = \frac{1}{N} \sum_{i=1}^N \sigma_{xx}(i) \quad (15)$$

where $\bar{\sigma}_{xx}$ is the averaged value of stress σ_{xx} , and N is the number of the stress nodal values at that depth.

Surface treatment of shot-peening is usually done to increase the strength of mechanical components of the metal. However, in many cases, there is the possibility of failure or alteration of the shot peened surface by surface defects such as micro-cracks and surface roughness defects [2, 3], which can significantly reduce the fatigue strength [40, 41]. Roughness defects are considered as a sequence of cavities due to shot-peening.

Roughness includes the arithmetical mean deviation of the profile Ra and the mean height of the five dominant peaks and the five deep valleys Rc. The obtained data after Gaussian filtering steps represents the surface irregularity without the presence of the wave component. The displacement of the surface target in the mid line was selected as data. The developed MATLAB routine provides the possibility of determining the parameters Ra, Rc according to their standard definitions presented.

Each factor is tested at three different levels, highest (1), medium (0) and lowest (-1). Their related levels are shown in real and coded values in Table 3.

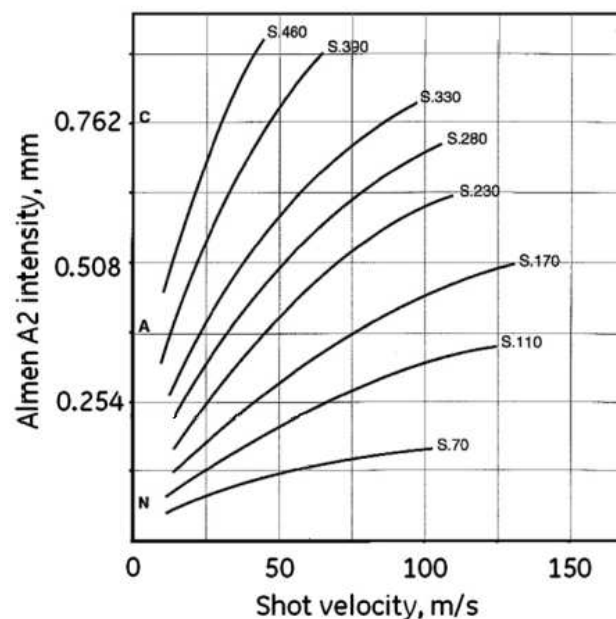


Fig. 2: Almen intensity vs. shot velocity for different shot sizes [38].



Table 4: The final matrix of the design of experiments and the results of the shot-peening simulation for various inputs

RUN	V (m/s)	d (mm)	C (%)	h (mm)	σ_{surf}^{RS} (MPa)	σ_{max}^{RS} (MPa)	δ_{max}^{RS} (mm)	δ_c^{RS} (mm)	Rc (μm)	Ra (μm)
1	110	0.7112	150	3	-737.0039	-1026.2839	0.1021	0.7718	11.4392	3.5075
2	90	0.5842	150	6	-715.3882	-988.7391	0.0721	0.5646	14.2873	3.6231
3	70	0.7112	150	6	-656.2845	-921.8067	0.0781	0.5826	11.9180	2.9833
4	70	0.5842	150	4.5	-751.2234	-992.5166	0.0676	0.4795	11.3565	3.4356
5	90	0.8382	200	4.5	-736.2363	-1094.0902	0.0991	0.8378	10.5295	4.1180
6	70	0.7112	100	4.5	-651.9672	-877.2058	0.0721	0.5586	11.6337	3.6414
7	90	0.7112	100	3	-711.8292	-971.2497	0.0781	0.6607	10.4972	3.3669
8	110	0.7112	100	4.5	-623.7722	-922.1007	0.1081	0.7613	15.1102	4.1356
9	90	0.5842	100	4.5	-644.9260	-909.4089	0.0766	0.5270	12.7927	3.2410
10	90	0.8382	150	3	-781.2282	-1057.9755	0.0841	0.7958	11.0446	3.6453
11	90	0.8382	150	6	-718.1584	-1035.4722	0.0961	0.8228	8.7978	2.8108
12	110	0.7112	150	6	-725.4332	-1042.3805	0.0901	0.8108	15.5082	3.9135
13	110	0.7112	200	4.5	-685.3791	-1060.1887	0.0991	0.8468	12.8203	3.9938
14	110	0.8382	150	4.5	-694.3964	-1004.2666	0.0766	0.9820	10.9870	3.6347
15	110	0.5842	150	4.5	-661.4981	-999.0297	0.0901	0.6532	11.3024	3.6695
16	70	0.8382	150	4.5	-761.6092	-1012.6668	0.0766	0.6802	10.1129	2.8386
17	90	0.7112	150	4.5	-735.9481	-1011.8378	0.0811	0.6982	12.8038	3.3431
18	90	0.7112	200	3	-883.7832	-1190.5149	0.0841	0.7177	11.2354	3.2967
19	90	0.7112	100	6	-692.8838	-955.4292	0.0781	0.6547	10.3430	2.9266
20	90	0.5842	200	4.5	-752.6129	-1036.9222	0.0721	0.5631	11.0186	3.3099
21	70	0.7112	200	4.5	-750.4079	-1030.2889	0.0721	0.5901	9.6687	3.3144
22	70	0.7112	150	3	-774.0852	-1005.7000	0.0721	0.5556	7.7528	2.6836
23	90	0.8382	100	4.5	-724.7551	-975.4200	0.0856	0.7748	14.1629	3.4474
24	90	0.5842	150	3	-744.8544	-981.5827	0.0721	0.5526	12.0294	3.3168
25	90	0.7112	200	6	-787.0832	-1068.1596	0.0781	0.7628	13.5839	3.5489

3.3 Optimization using desirability function approach

One of the most commonly used methods to simultaneously optimize the multiple responses is the desirability function approach to convert a multi-response problem to single response using mathematical transformations. In desirability function approach, the goal is to determine the values of the input variables, so that, firstly, all responses have a desirability greater than zero, and secondly, the overall desirability is maximal. Switch and Deringer [42] introduce a proper form of desirability functions that gives a score to each response, and adjusts the input parameters to maximize the total score. To define desirability function approach, each of the n response variables is assumed to depend on k independent input variable through Eq. 16:

$$y_i = f_i(x_1, x_2, \dots, x_k) + \epsilon_i \quad i = 1, 2, \dots, n \tag{16}$$

here, y_i , is the i-th variable of response, f_i is the relationship between this and the input variables (here shot-peening parameters) and ϵ_i is the error. In desirability function d, a value between 0 and 1 is assigned to each response variable y_i . The value 1 shows that the response variable is at the ideal endpoint (target) and 0 indicates the worst case of desirability for the response variable. The value of d increases with the optimization of the corresponding response. Depending on the goal of maximizing, minimizing, or achieving a certain value, various desirability functions can be defined. If the goal is to maximize the desirability function:

$$d_i = \begin{cases} 0 & \text{if } y_i \leq L_i \\ \left(\frac{y_i - L_i}{T_i - L_i}\right)^r & \text{if } L_i < y_i < T_i \\ 1 & \text{if } y_i \geq T_i \end{cases} \tag{17}$$

In the case of minimizing the target:

$$d_i = \begin{cases} 1 & \text{if } y_i \leq T_i \\ \left(\frac{y_i - U_i}{T_i - U_i}\right)^r & \text{if } T_i < y_i < U_i \\ 0 & \text{if } y_i \geq U_i \end{cases} \tag{18}$$



Table 5: The results of ANOVA analysis of surface residual stresses (σ_{surf}^{RS}) in the simulation of the shot-peening process to determine the effect of various parameters

Source	Sum of square	df	Mean Square	F-value	p-value	
Model	40017.95	4	10004.49	5.99	0.0025	significant
V	3963.76	1	3963.76	2.37	0.1392	insignificant
d	1773.42	1	1773.42	1.06	0.3152	insignificant
C	24785.61	1	24785.61	14.83	0.0010	significant
h	9495.16	1	9495.16	5.68	0.0272	significant
Residual	33417.73	20	1670.89			
Cor Total	73435.68	24				

Table 6: The results of ANOVA analysis of the maximum compressive stress (σ_{max}^{RS}) in the simulation the shot-peening process to determine the effects of various parameters

Source	Sum of square	df	Mean Square	F-value	p-value	
Model	77032.69	4	19258.17	15.81	< 0.0001	Significant
A-V	3818.66	1	3818.66	3.14	0.0918	insignificant
B-d	6151.38	1	6151.38	5.05	0.0361	Significant
C-C	62980.80	1	62980.80	51.71	< 0.0001	Significant
D-h	4081.86	1	4081.86	3.35	0.0821	insignificant
Residual	24357.96	20	1217.90			
Cor Total	1.014E+05	24				

Table 7: The results of ANOVA analysis of maximum compressive stress depth in the simulation the shot-peening process to determine the effects of various parameters

Source	Sum of square	df	Mean Square	F-value	p-value	
Model	0.0017	4	0.0004	7.10	0.0010	significant
A-V	0.0014	1	0.0014	22.15	0.0001	significant
B-d	0.0004	1	0.0004	6.21	0.0216	significant
C-C	3.006E-06	1	3.006E-06	0.0490	0.8270	insignificant
D-h	2.168E-19	1	2.168E-19	3.538E-15	1.0000	insignificant
Residual	0.0012	20	0.0001			
Cor Total	0.0030	24				

Table 8: The results of ANOVA analysis of compressive stress depth (δ_c^{RS}) in the simulation the shot-peening process to determine the effects of various parameters

Source	Sum of Squares	df	Mean Square	F-value	p-value	
Model	0.3793	10	0.0379	183.35	< 0.0001	significant
A-V	0.1586	1	0.1586	766.44	< 0.0001	significant
B-d	0.2011	1	0.2011	972.22	< 0.0001	significant
C-C	0.0121	1	0.0121	58.59	< 0.0001	significant
D-h	0.0017	1	0.0017	8.37	0.0118	significant
AB	0.0041	1	0.0041	19.84	0.0005	significant
AC	0.0007	1	0.0007	3.53	0.0812	insignificant
AD	0.0000	1	0.0000	0.1744	0.6826	insignificant
BC	0.0002	1	0.0002	0.8827	0.3634	insignificant
BD	0.0001	1	0.0001	0.2725	0.6099	insignificant
CD	0.0007	1	0.0007	3.15	0.0977	insignificant
Residual	0.0029	14	0.0002			
Cor Total	0.3822	24				

L_i , U_i and T_i are the lower, upper and target value respectively and r_i coefficient is determined by the user and determines how important it is to hit the target value. If $r_i = 1$, then the desirability function increases linearly. For $r_i < 1$, the desirability function is convex and concave for $r_i > 1$. Generally, r_i is considered one. In the maximum case, T_i interpreted as a large enough value for the response. In the minimum case, T_i denoting a small enough value for the response. After the desirability values for each response variable are calculated, they are combined in the form of the unit desirability function, which this final desirability function is calculated in Eq. 19:



$$D = \left(\prod_{i=1}^n d_i \right)^{\frac{1}{n}} \quad (19)$$

here, D is the final desirability function, d_i is the individual desirability function of each response variable, and n is the number of response variables. Now D must be maximized. The desirability approach consists of the following steps:

1. Simulate the shot-peening process and obtain response models using DoE for all six responses;
2. Define individual desirability functions for each intended response;
3. Maximize the overall desirability D with respect to the controllable factors.

4. Results

The results of FEM simulation for various parameters according to the Box-Behnken design are shown in Table 4. The statistical analysis of results is done with Design Expert 11 software. Analysis of variance (ANOVA) uses P-value in order to check the significance of the model and the effects of the independent variables on the responses. The P-value less than 0.05 indicates a significant result [43]. If the term shows a P-value higher than 0.05, it means that, the term in the model can be ignored.

4.1 The mathematical model of the surface stress

The recommended model is a linear model for surface stress (σ_{surf}^{RS}). The effects of shot-peening parameters are shown in Table 5 for σ_{surf}^{RS} . By examining the values of p-value for different terms, one can conclude that the effective parameters are C and h, respectively. V and d have less effect than other parameters. The obtained model for σ_{surf}^{RS} is determined in:

$$\sigma_{surf}^{RS} = -672.15 - 0.9089C + 18.7529h \quad (20)$$

It can be seen from the Eq. 20 that in addition to the coverage percentage, the sample thickness is also effective on the value of σ_{surf}^{RS} . The effect of thickness is to reduce compressive stress. Fig. 3 shows 3D surface plot of σ_{surf}^{RS} versus the input parameters. It shows that the parameter C has the greatest impact.

4.2 The mathematical model of the maximum compressive stress

Similarly, for other responses, suitable models can be obtained by software. The mathematical relation of appropriate model for maximum compressive stress (σ_{max}^{RS}) is linear and ANOVA analysis is presented in Table 6. The effective parameters are C and d respectively. V and h have less effect than C and d. The obtained model is:

$$\sigma_{max}^{RS} = -662.72 - 1.4489C - 178.276d \quad (21)$$

The effect of C and d are to increase compressive stress. Fig. 3 shows 3D surface plot of σ_{max}^{RS} versus the input parameters. The Fig. 4 shows that the parameter C has the greatest impact.

4.3 The mathematical model of the depth of the maximum compressive stress

The appropriate model for the depth of the maximum compressive stress (δ_{max}^{RS}) is linear as well. The corresponding ANOVA analysis is presented in Table 7. It can be seen that the effective parameters are V and d. The thickness h has no effect on δ_{max}^{RS} . The resulting model is expressed as Eq. 22:

$$\delta_{max}^{RS} = 0.003071 + 0.000532V + 0.04434d \quad (22)$$

Fig. 5 shows 3D surface plot of δ_{max}^{RS} versus the input parameters. It shows that the parameter V and d have the greatest impact.

4.4 The mathematical model of the compressive stress depth

The suitable model for compressive stress depth (δ_c^{RS}) is 2FI and the corresponding ANOVA is presented in Table 8. It is seen that the effective linear parameters are respectively d, V, C, h and the nonlinear effective parameter is V×d, respectively, and the resulting model is:

$$\delta_c^{RS} = 0.12183 - 0.003222V - 0.1157d + 0.00636C + 0.00801h + 0.01261Vd \quad (23)$$

Unlike δ_{max}^{RS} , δ_c^{RS} depend on h. The Eq. 23 shows that the δ_c^{RS} has a complex relationship with different parameters. Fig. 6 shows 3D surface plot of δ_c^{RS} versus the input parameters. It shows that the parameter d and V have the greatest impact.

4.5 The mathematical model of the roughness Ra

The recommended model is a linear model for roughness Ra. In Table 9 the effects of shot-peening parameters is observed for Ra. By examining p-value for different terms, it is concluded that the effective parameter is V, and other parameters have a small effect on Ra. h and d have less effect than other parameters. The model obtained for Ra is expressed as:

$$Ra = 1.9457 + 0.01649V \quad (24)$$

Fig. 7 shows 3D surface plot of roughness Ra versus the input parameters. The Fig. 7 shows that the parameter V has the greatest impact.



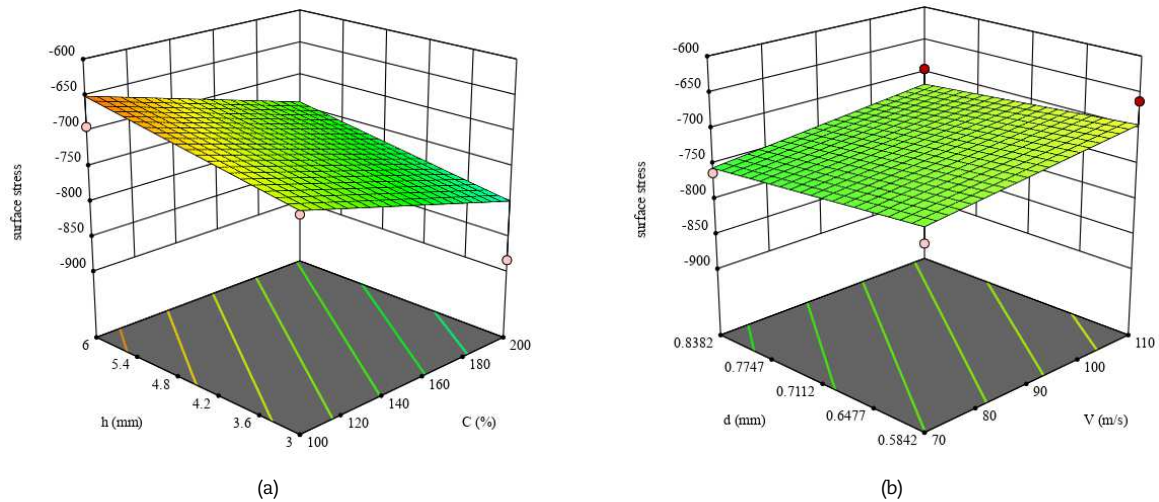


Fig. 3: 3D surface plot of surface stress versus a) coverage and target thickness b) shot velocity and shot diameter.

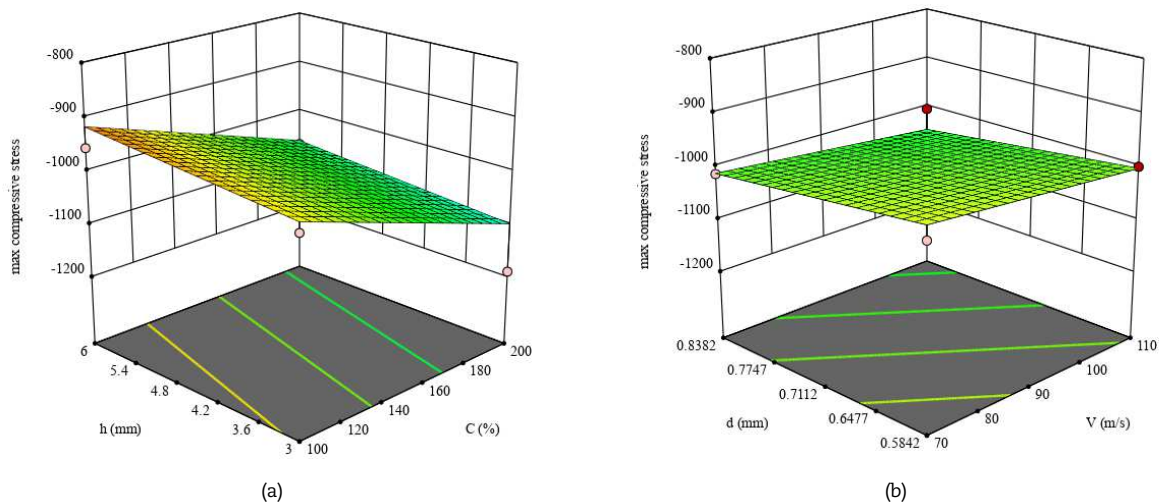


Fig. 4: 3D surface plot of max compressive stress versus a) coverage and target thickness b) shot velocity and shot diameter.

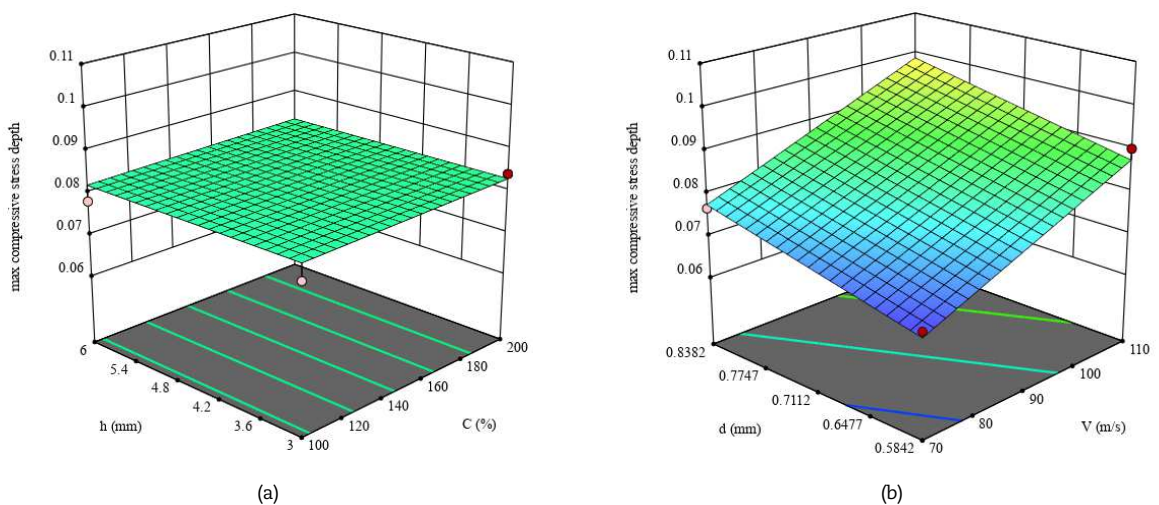


Fig. 5: 3D surface plot of max compressive stress depth versus a) coverage and target thickness b) shot velocity and shot diameter.



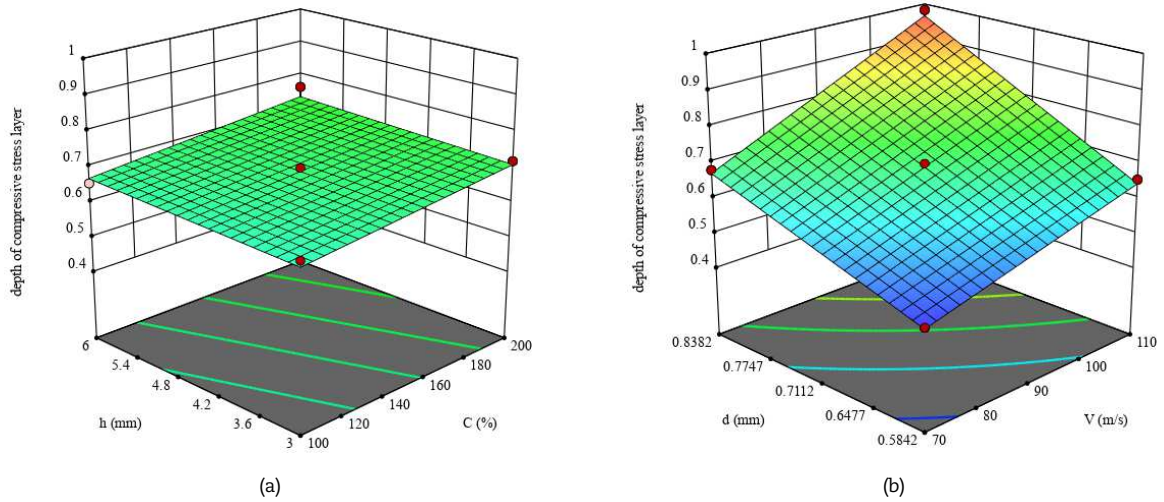


Fig. 6: 3D surface plot of depth of compressive stress layer versus a) coverage and target thickness b) shot velocity and shot diameter.

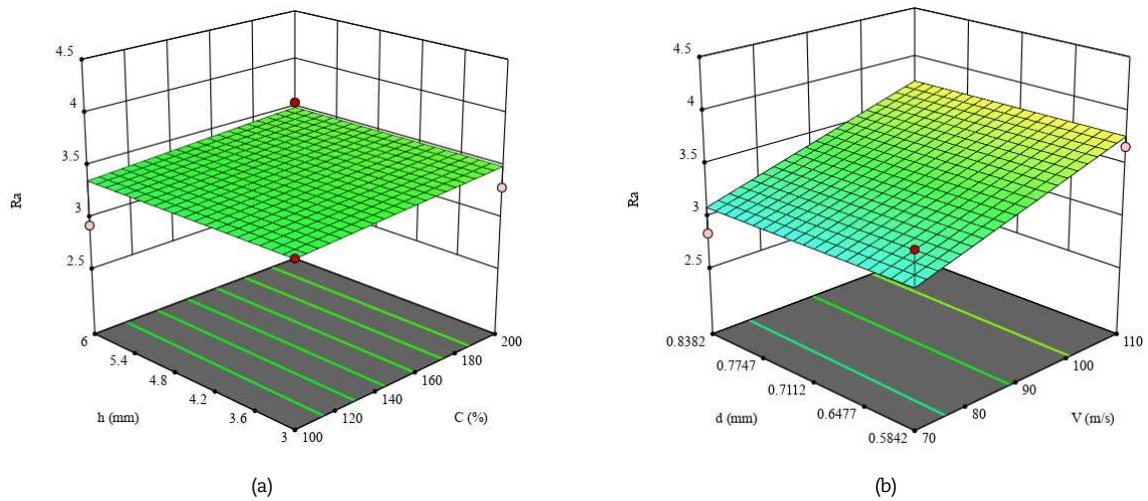


Fig. 7: 3D surface plot of roughness Ra versus a) coverage and target thickness b) shot velocity and shot diameter.

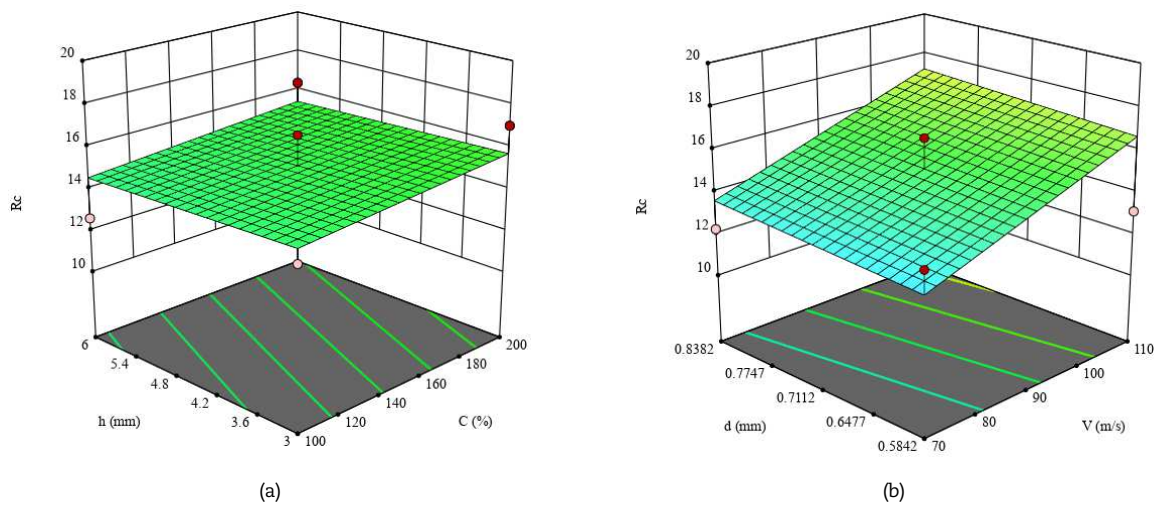


Fig. 8: 3D surface plot of roughness Rc versus a) coverage and target thickness b) shot velocity and shot diameter.



Table 9: The results of the ANOVA analysis of roughness Ra in the simulation the shot-peening process to determine the effects of various parameters

Source	Sum of Squares	df	Mean Square	F-value	p-value	
Model	1.36	4	0.3406	3.02	0.0424	significant
A-V	1.31	1	1.31	11.57	0.0028	significant
B-d	0.0009	1	0.0009	0.0075	0.9316	insignificant
C-C	0.0564	1	0.0564	0.4999	0.4877	insignificant
D-h	9.363E-06	1	9.363E-06	0.0001	0.9928	insignificant
Residual	2.26	20	0.1129			
Cor Total	3.62	24				

Table 10: The results of ANOVA analysis of roughness Rc in simulation of shot-peening process to determine the effects of various parameters

Source	Sum of Squares	df	Mean Square	F-value	p-value	
Model	42.18	4	10.54	2.89	0.0485	significant
A-V	38.82	1	38.82	10.66	0.0039	significant
B-d	0.9672	1	0.9672	0.2655	0.6120	insignificant
C-C	2.08	1	2.08	0.5706	0.4588	insignificant
D-h	0.3088	1	0.3088	0.0848	0.7739	insignificant
Residual	72.85	20	3.64			
Cor Total	115.03	24				

Table 11: Optimal shot-peening parameters for different target functions

	Objective function	Optimum parameter			Optimum value
		V(m/s)	d(mm)	C(%)	
1	σ_{surf}^{RS}	-	-	200	-760.18 MPa
2	σ_{max}^{RS}	-	0.8382	200	-1101.93 MPa
3	δ_{max}^{RS}	110	0.8382	-	0.099 mm
4	δ_c^{RS}	110	0.8382	200	1 mm
5	Ra	70	-	-	3.1 μ m
6	Rc	70	-	-	13.33 μ m

Table 12: Optimal shot-peening parameters for multiple target functions

	Objective function 1	Objective function 2	Optimum parameter			Optimum value 1	Optimum value 2
			V(m/s)	d(mm)	C(%)		
1	σ_{surf}^{RS}	Ra	70	-	200	-760.18 MPa	3.1 μ m
2	σ_{max}^{RS}	Ra	70	0.8382	200	-1101.93 MPa	3.1 μ m
3	δ_{max}^{RS}	Rc	98.03	0.8382	-	0.092 mm	15.67 μ m
4	δ_c^{RS}	Rc	96.22	0.8382	200	0.836 mm	15.5 μ m

Table 13: Optimal shot-peening parameters for all target functions

	Objective functions	Optimum parameter			σ_{surf}^{RS}	σ_{max}^{RS}	δ_{max}^{RS}	δ_c^{RS}	Ra	Rc
		V(m/s)	d(mm)	C(%)						
1	All responses	90.12	0.8382	200	-760.18	-1101.93	0.088	0.85	3.43	15.79

4.6 The mathematical model of the roughness Rc

Similarly, ANOVA analysis can be performed for Rc roughness. The selected model for Rc is a linear model and the corresponding ANOVA is given in Table 10. It is again seen that V is an effective parameter and the resulting model is expressed as Eq. 25:

$$Rc = 7.035 + 0.08993 V \tag{25}$$

Fig. 8 shows 3D surface plot of roughness Rc versus the input parameters. It can be seen that the parameter V has the greatest impact.



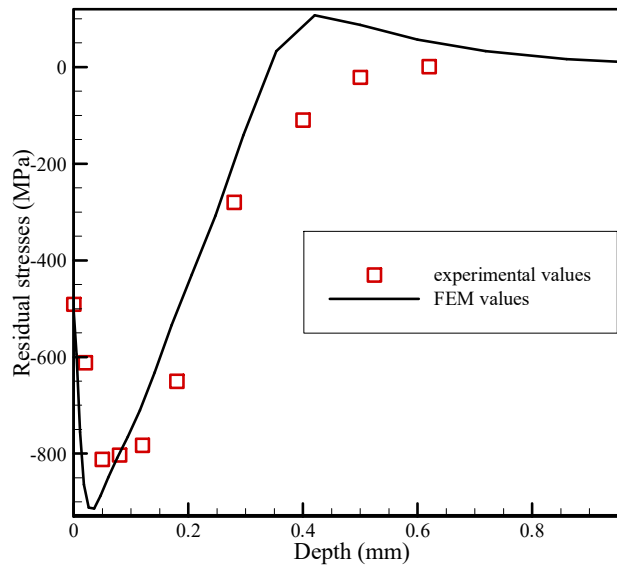


Fig. 9: Residual-stress profiles in-depth of shot-peened AISI 420.

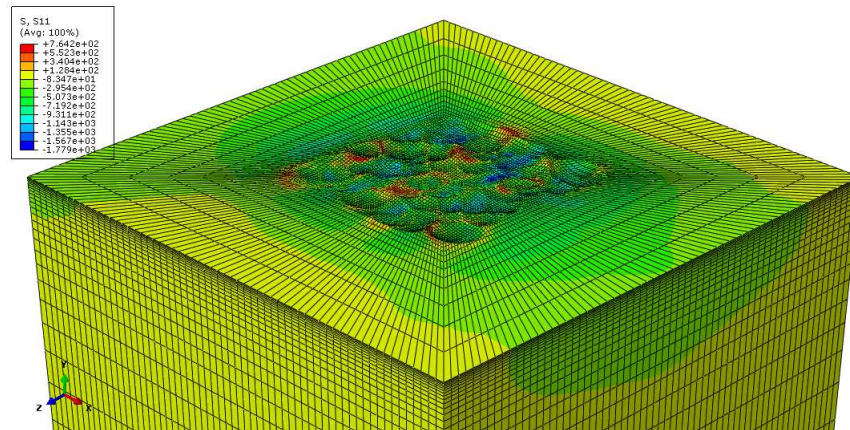


Fig. 10: Stress contour (S11) of shot peened surface

4.7 Optimization

According to the results and models shown in the previous section, one can see the effects of the input parameters on the output response and obtain optimal point. According to the model presented for each quantity, the optimal value for a constant thickness of 5mm is given in Table 11. The compressive stresses and depths should be maximized, whereas roughness must be minimized.

Note that the optimal values obtained in Table 11 are considered as single objective, so the optimal values for each quantity can refuse to be the optimal point for other quantities. Such a situation is not desirable because the increase in the fatigue life of the part depend the compressive residual stress and roughness simultaneously, and if only one of the responses is optimal, fatigue life may not improve or even decrease. Thus, it is important to optimize simultaneous responses in multi-objective optimizations. In doing so, different modes are considered as seen in Table 12. To demonstrate the effects of shot-peening on surface integrity, multi-objective optimization is done for all responses simultaneously and shown in Table 13.

5. Validation and Discussion

In this section, the models obtained from the results section are validated and compared with the experimental data. The operating conditions are as:

(i) Shot S170, (ii) Intensity Almen 14A, (equivalent to velocity 67.7 m/s), (iii) Coverage 100%, (iv) Impact angles 90 degree.

The coefficient of friction μ between the shots and the surface during the contact is 0.2.

Fig. 9 shows the comparison between the XRD experimental results and the residual compressive stress profile obtained numerically. XRD residual stress analysis and the electrolytic layer removal technique were used to obtain residual stress depth profiles. Stress relaxation due to layer removal was not taken into account, since the affected region was small and no significant relaxation effects could be expected. Residual stresses were calculated for the plain stress condition. A satisfactory correspondence is observed between the calculated results and experimental values. Fig. 10 shows the contour of the stress S11.



To compare the numerical results of this study with the experimental data of other papers, the relation between the Almen intensity and velocity can be used. As regards Almen intensity in the finite intervals is linear in relation to velocity, it follows that $\sigma_{\text{surf}}^{\text{RS}}$ is very low dependency to Almen intensity, which means the final effect of shot-peening on $\sigma_{\text{surf}}^{\text{RS}}$ is strongly dependent on the properties of the material itself. This result is consistent with the experimental results of ref. [44] and their empirical formulas for AISI 4340 steel, and both steel behave the same. The direct relationship between stress and coverage percentage as the most important factor has been seen in experiment data in ref. [45] too. It may be possible that different steels have similar behavior to the shot-peening parameters that should be investigated in the future.

It can be seen that $\sigma_{\text{max}}^{\text{RS}}$ have a very low dependence on the shot velocity and Almen intensity. A similar behavior is found in the empirical equations of ref. [44] for $\sigma_{\text{max}}^{\text{RS}}$.

The $\sigma_{\text{max}}^{\text{RS}}$ has a linear relationship with velocity and consequently with Almen intensity. This equation is also in consistent with the empirical formula given in reference [44].

The δ_c^{RS} has a linear relationship with velocity and hence Almen intensity. As in Eq. 18, this equation is consistent with the empirical formula in reference [44]. The relation of δ_c^{RS} with different parameters is mentioned in references [46,47].

Equation 20 shows that Ra highly depends on the velocity of the shot and, consequently, is equal to that of Almen intensity. The results of this simulation are confirmed with the experimental results presented in reference [44].

It is seen here that Rc has a high dependence on velocity and less dependence on the other parameter.

It is seen from Table 12 that the optimal parameters for simultaneous optimization of surface compressive stress and Ra are the same with case that surface stress optimized with low velocity. The reason is that the surface stress is dependent on the coverage of C, whereas Ra depends on the velocity, so with high C and low velocity we can achieve optimal point. The results of optimizing the maximum compressive stress and Ra are as before. Because the dependency of maximum compressive stress with the velocity is also very low, and the main parameter is the coverage C, it can be concluded that with high C and low velocity, the surface stress, the maximum compressive stress and Ra are optimum. In other cases, the results are different from the single-objective mode that the designer can select one of them depending on his needs. In general, the most important parameter of the residual stresses is coverage C, while for the other four responses, velocity V is important, so to optimize all responses at the same time, high coverage is still obtained, but speed is needed to obtain again. Of course, the optimization process is performed in the levels that show in table 3 in this study and the results may be changed if the levels change or there is maybe minimum value for the velocity and maximum value for the C thus further investigates needed to be done.

6. Conclusion

The paper presented suitable and reliable methods to study and optimize the response variables (residual stress and surface roughness) simultaneously to determine the optimal parameters of the shot-peening process. The main results are as follows:

1. The compressive residual stress, plastic strain, and roughness parameter for different shot-peening conditions can be predicted using our proposed model.
2. By simulating the shot-peening process it was clarified that:
 - The surface residual stress is independent of shot velocity and size, but depends on the coverage and sample thickness.
 - The maximum residual stress is independent of shot velocity and sample thickness, but depends on the coverage and the diameter of the shot.
 - The depth of maximum compressive stress is directly related to the velocity and diameter of the shot.
 - The depth of compressive stress depends on all of studied parameters i.e. the diameter of the shot, shot velocity, coverage and sample thickness.
 - Roughness has a linear relationship with shot velocity.
 - In other words, surface stress and maximum residual stress are independent of shot velocity and other parameters are directly related to shot velocity.
3. As one of the common applications of shot-peening is to increase fatigue life, simultaneous attention to inductive compressive stress and roughness caused by shot-peening is important. Therefore, multi-objective optimization methods are recommended.
4. With high-coverage and low-velocity, one can reach optimal conditions for surface stress, maximum compressive stress, and roughness of Ra simultaneously.

Author Contributions

All authors discussed the results, reviewed, and approved the final version of the manuscript.

Acknowledgments

Not applicable.

Conflict of Interest

The authors declared no potential conflicts of interest with respect to the research, authorship, and publication of this article.

Funding

The authors received no financial support for the research, authorship, and publication of this article.

Data Availability Statements

The datasets generated and/or analyzed during the current study are available from the corresponding author on reasonable request.



References

- [1] Society of Automotive Engineers Handbook: SAE Publications, 1986.
- [2] R. Fathallah, H. Sidhom, C. Braham, and L. Castex, Effect of surface properties on high cycle fatigue behaviour of shot peened ductile steel, *Materials Science and Technology*, 19, 2003, 1050-1056.
- [3] A. Eleiche, M. Megahed, and N. Abd-Allah, The shot-peening effect on the HCF behavior of high-strength martensitic steels, *Journal of Materials Processing Technology*, 113, 2001, 502-508.
- [4] D. Hills, R. Waterhouse, and B. Noble, An analysis of shot-peening, *The Journal of Strain Analysis for Engineering Design*, 18, 1983, 95-100.
- [5] Y. Al-Obaid, Shot-peening mechanics: experimental and theoretical analysis, *Mechanics of Materials*, 19, 1995, 251-260.
- [6] S. Al-Hassani, Mechanical aspects of residual stress development in shot-peening, *Shot-peening*, 583, 1981.
- [7] M. Obata and A. Sudo, Effect of shot-peening on residual stress and stress corrosion cracking for cold worked austenitic stainless steel, in *Proceedings of the ICSP-5 Conference*, Oxford, UK, 1993.
- [8] T. Dorr, M. Hilpert, P. Beckmerhagen, A. Kiefer, and L. Wagner, Influence of shot-peening on fatigue performance of high-strength aluminum-and magnesium alloys, 7th ICSP, American Shot-peening Society, 1999.
- [9] A. A. Ahmed, M. Mhaede, M. Basha, M. Wollmann, and L. Wagner, The effect of shot-peening parameters and hydroxyapatite coverage on surface properties and corrosion behavior of medical grade AISI 316L stainless steel, *Surface and Coatings Technology*, 280, 2015, 347-358.
- [10] S. Mahagaonkar, P. Brahmankar, and C. Seemikeri, Effect of shot-peening parameters on microhardness of AISI 1045 and 316L material: an analysis using design of experiment, *The International Journal of Advanced Manufacturing Technology*, 38, 2008, 563-574.
- [11] Y.-S. Nam, Y.-I. Jeong, B.-C. Shin, and J.-H. Byun, Enhancing surface layer properties of an aircraft aluminum alloy by shot-peening using response surface methodology, *Materials & Design*, 83, 2015, 566-576.
- [12] T. Hong, J. Ooi, and B. Shaw, A numerical simulation to relate the shot-peening parameters to the induced residual stresses, *Engineering Failure Analysis*, 15, 2008, 1097-1110.
- [13] S. Meguid, G. Shagal, J. Stranart, and J. Daly, Three-dimensional dynamic finite element analysis of shot-peening induced residual stresses, *Finite Elements in Analysis and Design*, 31, 1999, 179-191.
- [14] M. Guagliano, Relating Almen intensity to residual stresses induced by shot-peening: a numerical approach, *Journal of Materials Processing Technology*, 110, 2001, 277-286.
- [15] T. Kim, J. H. Lee, H. Lee, and S.-k. Cheong, An area-average approach to peening residual stress under multi-impacts using a three-dimensional symmetry-cell finite element model with plastic shots, *Materials & Design*, 31, 2010, 50-59.
- [16] W. Cheng, H. Jiacheng, G. Zhenbiao, X. Yangjian, and W. Xiaogui, Simulation on Residual stress of shot-peening Based on a Symmetrical cell model, *Chinese Journal of Mechanical Engineering*, 30, 2017, 344-351.
- [17] S. Meguid, G. Shagal, and J. Stranart, Development and validation of novel FE models for 3D analysis of peening of strain-rate sensitive materials, *Journal of Engineering Materials and Technology*, 129, 2007, 271-283.
- [18] A. Ghasemi, S. M. Hassani-Gangaraj, A. Mahmoudi, G. Farrahi, and M. Guagliano, Shot-peening coverage effect on residual stress profile by FE random impact analysis, *Surface Engineering*, 32, 2016, 861-870.
- [19] H. Miao, S. Larose, C. Perron, and M. Lévesque, On the potential applications of a 3D random finite element model for the simulation of shot-peening, *Advances in Engineering Software*, 40, 2009, 1023-1038.
- [20] A. Mahmoudi, A. Ghasemi, G. Farrahi, and K. Sherafatnia, A comprehensive experimental and numerical study on redistribution of residual stresses by shot-peening, *Materials & Design*, 90, 2016, 478-487.
- [21] Y.-S. Nam, U. Jeon, H.-K. Yoon, B.-C. Shin, and J.-H. Byun, Use of response surface methodology for shot-peening process optimization of an aircraft structural part, *The International Journal of Advanced Manufacturing Technology*, 87, 2016, 2967-2981.
- [22] A. AlSumait, Y. Li, M. Weaser, K. Niji, G. Battel, R. Toal, et al., A Comparison of the Fatigue Life of Shot-Peened 4340M Steel with 100, 200, and 300% Coverage, *Journal of Materials Engineering and Performance*, 28, 2019, 1780-1789.
- [23] F. Petit-Renaud, J. Evans, A. Metcalfe, and B. Shaw, Optimization of a shot-peening process, *Proceedings of the Institution of Mechanical Engineers, Part L: Journal of Materials: Design and Applications*, 222, 2008, 277-289.
- [24] J. S. Romero, E. Rios, Y. Fam, and A. Levers, *Optimisation of the shot-peening process in terms of fatigue resistance*, University of Sheffield, 2002.
- [25] P. George, N. Pillai, and N. Shah, Optimization of shot-peening parameters using Taguchi technique, *Journal of Materials Processing Technology*, 153, 2004, 925-930.
- [26] A. Vielma, V. Llana, and F. Belzunce, Shot-peening intensity optimization to increase the fatigue life of a quenched and tempered structural steel, *Procedia Engineering*, 74, 2014, 273-278.
- [27] O. Unal, Optimization of shot-peening parameters by response surface methodology, *Surface and Coatings Technology*, 305, 2016, 99-109.
- [28] B. Bhuvrangan, S. M. Srinivasan, B. Maffeo, and O. Prakash, Constrained probabilistic multi-objective optimization of shot-peening process, *Engineering Optimization*, 43, 2011, 657-673.
- [29] S. Baragetti, Shot-peening optimisation by means of DOE: Numerical simulation and choice of treatment parameters, *International Journal of Materials and Product Technology*, 12, 1997, 83-109.
- [30] O. Unal and E. Maleki, Shot-peening optimization with complex decision-making tool: Multi criteria decision-making, *Measurement*, 125, 2018, 133-141.
- [31] R. Seddik, A. Bahloul, A. Atig, and R. Fathallah, A simple methodology to optimize shot-peening process parameters using finite element simulations, *The International Journal of Advanced Manufacturing Technology*, 90, 2017, 2345-2361.
- [32] T. Kim, H. Lee, S. Jung, and J. H. Lee, A 3D FE model with plastic shot for evaluation of equi-biaxial peening residual stress due to multi-impacts, *Surface and Coatings Technology*, 206, 2012, 3125-3136.
- [33] S.M.H. Gangaraj, M. Guagliano, and G. H. Farrahi, An approach to relate shot peening finite element simulation to the actual coverage, *Surface and Coatings Technology*, 243, 2014, 39-45.
- [34] T. Kim, H. Lee, H.C. Hyun, and S. Jung, Effects of Rayleigh Damping, Friction and Rate-Dependency on 3D Residual Stress Simulation of Angled Shot Peening, *Materials & Design*, 46, 2013, 26-37.
- [35] F. Yang, and G. Yukui, Predicting the peen forming effectiveness of Ti-6Al-4V strips with different thicknesses using realistic finite element simulations, *Journal of Engineering Materials and Technology*, 138, 2016, 011004.
- [36] D. Kirk, Theoretical principles of shot-peening coverage, *Shot Peener*, 19, 2005, 24.
- [37] D. C. Montgomery, *Statistical quality control*, vol. 7, Wiley, New York, 2009.
- [38] Shotpeener Company, Shot size and speed to achieve Almen intensity, <http://www.shotpeener.com/learning/ref.phpS>.
- [39] A. Gariépy, H.Y. Miao, and M. Lévesque, Simulation of the shot peening process with variable shot diameters and impacting velocities, *Advances in Engineering Software*, 114, 2017, 121-133.
- [40] L. Wagner, Mechanical surface treatments on titanium, aluminum and magnesium alloys, *Materials Science and Engineering: A*, 263, 1999, 210-216.
- [41] ENISO, Geometrical Product Specifications (GPS)–Surface Texture: Profile Method–Terms, Definitions and Surface Texture Parameters, 1997.
- [42] G. Derringer and R. Suich, Simultaneous optimization of several response variables, *Journal of Quality Technology*, 12, 1980, 214-219.
- [43] D. S. Moore, G. P. McCabe, B. A. Craig, *Introduction to the Practice of Statistics*, 6th ed., W.H. Freeman and Company, 2009.
- [44] V. Llana and F. Belzunce, Study of the effects produced by shot-peening on the surface of quenched and tempered steels: roughness, residual stresses and work hardening, *Applied Surface Science*, 356, 2015, 475-485.
- [45] X. Wang, W. Zhou, G. Wu, J. Gan, Y. Yang, H. Huang, J. He, and H. Zhong, Combining the finite element method and response surface methodology for optimization of shot peening parameters, *International Journal of Fatigue*, 129, 2019, 105231.
- [46] K. A. Soady, B.G. Mellor, G. D. West, G. Harrison, A. Morris, and P. A. S. Reed, Evaluating surface deformation and near surface strain hardening resulting from shot peening a tempered martensitic steel and application to low cycle fatigue, *International Journal of Fatigue*, 54, 2013, 106-117.
- [47] S. Srilakshmi, D. V. Vidyasagar, and S. Devaki Rani, The Role of Residual Stresses with Various Shot Peening Parameters on 12%Cr Blading Steel for LP Turbine Applications, *International Journal of Mechanical Engineering and Robotics Research*, 1(1), 2013, 90-96.





© 2022 Shahid Chamran University of Ahvaz, Ahvaz, Iran. This article is an open access article distributed under the terms and conditions of the Creative Commons Attribution-NonCommercial 4.0 International (CC BY-NC 4.0 license) (<http://creativecommons.org/licenses/by-nc/4.0/>).

How to cite this article: Hassanzadeh M., Moussavi Torshizi S.E. Multi-objective Optimization of Shot-peening Parameters using Design of Experiments and Finite Element Simulation: A Statistical Model, *J. Appl. Comput. Mech.*, 8(3), 2022, 838–852. <https://doi.org/10.22055/JACM.2020.33102.2152>

Publisher's Note Shahid Chamran University of Ahvaz remains neutral with regard to jurisdictional claims in published maps and institutional affiliations.

